

SCOUR DEVELOPMENT DOWNSTREAM OF APRONS WITH AND WITHOUT END-SILL

Giuseppe Oliveto¹

¹Department of Environmental Engineering and Physics, University of Basilicata, Italy, Viale dell'Ateneo 10, I-85100 Potenza
E-mail: giuseppe.oliveto@unibas.it

Abstract

This paper focuses on the local bed scour downstream of low-head spillways with stilling basins. Experiments were carried out in a 1 m wide rectangular channel. Free overfall jets from an ogee-crested spillway plunged into a positive-step stilling basin or a plain horizontal apron. Four nearly uniform bed sediments were used. All the experiments were performed under steady approach flow conditions and runs lasted three days on average to achieve a quasi-equilibrium state and well developed scour pits. Tail water depths were set to minimize the combination of local and general scour phenomena. Based on the experimental data, salient features on the spatial and temporal evolution of the local bed morphology are provided highlighting the effects of the end-sill. It was found that the main parameters governing the scouring process are the tailwater densimetric Froude number, the relative tailwater depth, and a dimensionless time. The temporal variation of the scour hole geometry can be estimated by using simple power-type equations that relate the scour geometry to the controlling scour parameters. Polynomial-type equations are also given for the temporal axial scour profiles.

Introduction

Stilling basins are commonly built to keep energy flows from scouring the streambed. However, the flow turbulence level within them is often high and local bed scour can develop. Though a number of studies on local scour below low-head spillways have been made, the results are still inconclusive mainly in regards to the spatial and temporal evolution of the local bed morphology. Literature reviews are given by Breusers and Raudkivi (1991), Hager (1992), Hoffmans and Verheij (1997), and Sarkar and Dey (2004). Breusers (1967) accomplished a wide-ranging work using various bed materials of different densities and geometric configurations. A formula for the temporal scour evolution was proposed. Kuti and Yen (1976) considered cohesive sediment beds analyzing the influence of clay minerals mixed with cohesionless soils. Numerous tests were carried out by Farhodi and Smith (1982; 1985) who used six different materials. Results were in agreement with those of Breusers (1967). Gisonni and Rasulo (1997) suggested an

approach to estimate the scour depth at the equilibrium stage as function of the turbulence intensity coefficient and the reduced critical velocity for the initiation of sediment transport. Dargahi (2003) made an experimental study to examine the similarity of scour profiles and the scour geometry. No experimental evidence was found in support of the similarity. Power-law type equations were introduced to predict the scour geometry. Adduce and Sciortino (2006) presented both numerical and experimental investigations on local scour downstream of a sill followed by a rigid apron. Adduce and La Rocca (2006) investigated the different scouring processes due to different jets developing downstream of a trapezoidal drop followed by a rigid apron. Farhodi, Hosseini, and Sedghi-Asl (2010) investigated the performance of a neuro-fuzzy model in estimating the properties of scour hole downstream of a U.S.B.R. Type I stilling basin. Results showed a significant agreement between estimated and experimental data. Finally, Pagliara and Palermo (2011) assessed the effect of both the width and length of stilling basins on scour features and flow pattern downstream of a block ramp. Overall, the above studies consider simplified stilling basins such as plain aprons without appurtenances. The present study, that follows previous contributions (Oliveto & Comuniello, 2009; Oliveto, Comuniello, & Bulbule, 2011), aims to highlight the main differences between the local bed morphology that develops downstream of a plain apron and that downstream of a more realistic stilling basin with an end-sill. The results would be useful for technical applications and the validation of numerical models.

Experiments

Experiments were carried out in a 1 m wide and 20 m long rectangular straight channel at the University of Basilicata, Italy. An ogee-crested spillway with stilling basin was placed in the channel 6 m from the inlet. The weir height above the downstream undisturbed bed level, w , was 0.20 m. Three stilling basins were tested. Two of them used a positive step at the end of the basin and their basin length, l , was 0.93 and 1.43 m. The other consisted of a plain apron with $l=1.65$ m. The end-sill height, s , was kept constant and equal to 0.092 m. Details on the first two stilling basins and the related experimental observations are given in

Oliveto *et al.* (2011), while details on the physical model with the plain apron and the related experimental data are provided in Oliveto (2012).

Four (almost) uniform bed sediments were used for the positive-step stilling basins. Namely, (i) sand with median grain size $d_{50}=1.7$ mm and sediment gradation $\sigma=(d_{84}/d_{16})^{0.5}=1.5$, (ii) sand with $d_{50}=2.5$ mm and $\sigma=1.2$, (iii) gravel with $d_{50}=9.0$ mm and $\sigma=1.5$, and (iv) lead spheres (of density $\rho_s=11400$ kg/m³) with $d_{50}=1.3$ mm and $\sigma=1.1$. Gravel was used to explore sediment grain size effects. Lead spheres were used to further investigate the role of the so-called densimetric Froude number. The same bed sediments, except lead spheres, were considered for the plain apron. The undisturbed bed surface was horizontal and flushed with the stilling basin end.

All the experiments were performed keeping constant over the time discharge and tailwater depth. Runs typically lasted three days to get quasi equilibrium conditions as well as well-deepen scour holes, but also some runs of short duration were performed to collect reliable experimental data at the earlier scour stages. Tailwater depths were set to minimize the overlapping of local and general scour phenomena. In general, undular hydraulic jumps developed when positive-step stilling basins were used while undular hydraulic jumps or hydraulic jumps (basically over the apron) formed when the plain apron was tested. Figure 1 shows the flow conditions for two runs with different stilling basin.

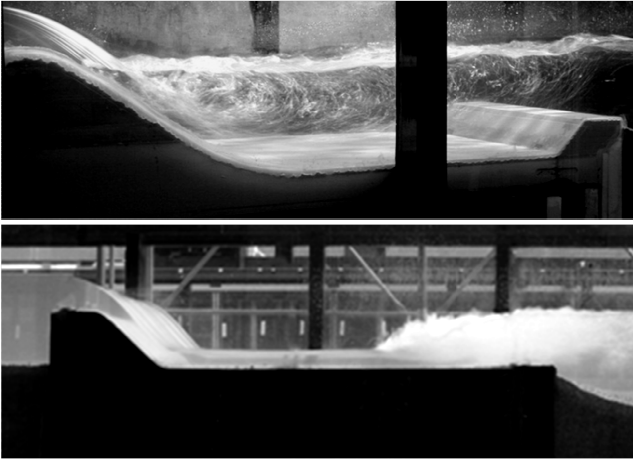


Figure 1: Flow features for two runs characterized by a positive-step stilling basin (photograph on the top) and a plain horizontal apron (photograph on the bottom).

The water discharge was measured with an orifice plate with accuracy of $\pm 3\%$. The water surface was measured with a conventional point gauge with accuracy to the nearest millimetre and the sediment surface with a shoe gauge. For the runs of long duration, flow depths and bed levels were usually measured at 2, 24, 48 hours from the start and at the end of the run. Bed level readings were

taken with water continuing to flow except for the last inspection that was done after stopping the flow.

Once the bed was accurately levelled, the channel was gradually filled submerging the working section with an adjustable sharp crested weir placed at the channel downstream end, avoiding in this way any sediment movement. The water discharge was then gradually increased and set to the pre-selected value. Finally, the experiment started when also the tailwater depth was set to the pre-selected value lowering the weir. Some photographs for run C16 are provided in Figure 2. They show hydraulic and bed morphology features with time. For this run a submerged hydraulic jump formed.



Figure 2: Hydraulic and bed morphology features with time for run C16 with discharge $Q=60$ l/s, tailwater depth $h_{tw}=0.21$ m and $d_{50}=1.7$ mm. Photographs from the top to the bottom refer to times $t=2, 12, 24, 48,$ and 72 hours from run starting.

Dimensional Analysis

For a given spillway, the axial maximum scour depth z can be expressed as function of the following independent variables

$$z = f_1(l, s, q, h_{tw}, \nu, \rho, d_{50}, \sigma, \rho_s, g, t) \quad (1)$$

with f_1 unspecified function, q overflow discharge per unit width, h_{tw} tailwater depth, ν kinematic viscosity, ρ water density, g gravitational acceleration, and t generic time. For two-phase flow phenomena involving sediment-water interaction, g , ρ , and ρ_s can be grouped into $g' = g(\rho_s - \rho)/\rho$. In turbulent flow, ν has small effect on scour and can be neglected. The application of the Buckingham π theorem yields

$$\frac{z}{h_{tw}} = f_2 \left(F_d, \frac{l}{h_{tw}}, \frac{s}{h_{tw}}, \frac{h_{tw}}{d_{50}}, \sigma, \frac{\sqrt{g'd_{50}}}{h_{tw}} t \right) \quad (2)$$

with f_2 unspecified function, and F_d tailwater densimetric Froude number = $V/(g'd_{50})^{0.5}$ with V cross sectional flow velocity. z/h_{tw} can be hypothesized to be proportional to the product of the powers of these dimensionless parameters as

$$\frac{z}{h_{tw}} = n_0 F_d^{n_1} \left(\frac{l}{h_{tw}} \right)^{n_2} \left(\frac{s}{h_{tw}} \right)^{n_3} \left(\frac{h_{tw}}{d_{50}} \right)^{n_4} \sigma^{n_5} T^{n_6} \quad (3)$$

with $n_0, n_1, n_2, n_3, n_4, n_5,$ and n_6 coefficients to be estimated and $T=(g'd_{50})^{0.5}t/h_{tw}$. Analogously, it can be assumed

$$\frac{x}{h_{tw}} = n_0 F_d^{n_1} \left(\frac{l}{h_{tw}} \right)^{n_2} \left(\frac{s}{h_{tw}} \right)^{n_3} \left(\frac{h_{tw}}{d_{50}} \right)^{n_4} \sigma^{n_5} T^{n_6} \quad (4)$$

$$\frac{\chi}{h_{tw}} = n_0 F_d^{n_1} \left(\frac{l}{h_{tw}} \right)^{n_2} \left(\frac{s}{h_{tw}} \right)^{n_3} \left(\frac{h_{tw}}{d_{50}} \right)^{n_4} \sigma^{n_5} T^{n_6} \quad (5)$$

whit x the horizontal distance from the stilling basin end of the site where z occurs and χ the axial scour hole length. Clearly, the parameter s/h_{tw} vanishes in case of plain apron.

Analysis of data

A multiple regression analysis according to Equations (3) to (5) yielded the results commented here below.

Characteristics of the scour hole

Oliveto *et al.* (2011) found that for apron with end-sill the most important parameters (ranked in order of relevance) are $F_d, T, \sigma,$ and h_{tw}/d_{50} , whereas the remainders s/h_{tw} and l/h_{tw} are less significant. The negligibility of s/h_{tw} was expected because s constant, while that of l/h_{tw} is in contrast with literature findings according to which the maximum scour depth increases with l decreasing (Dey & Sarkar, 2006). This can be probably due to the only two

values of l tested. In particular, the following equations were proposed to estimate $z, x,$ and χ

$$\frac{z}{h_{tw}} = 0.02 F_d^{2.32} \left(\frac{h_{tw}}{d_{50}} \right)^{-0.16} T^{0.21} \quad (6)$$

$$\frac{x}{h_{tw}} = 0.12 F_d^{2.73} \left(\frac{h_{tw}}{d_{50}} \right)^{-0.34} T^{0.18} \quad (7)$$

$$\frac{\chi}{h_{tw}} = 0.26 F_d^{3.27} \left(\frac{h_{tw}}{d_{50}} \right)^{-0.30} T^{0.17}. \quad (8)$$

They apply for $1.16 \leq F_d \leq 2.79,$ $4.4 \cdot 10^3 \leq T \leq 1.3 \cdot 10^6,$ and $16 \leq h_{tw}/d_{50} \leq 154.$ By using the same analysis in the case of the plain apron, it comes out that the most important parameters (ranked in order of importance) are $F_d, T, h_{tw}/d_{50},$ and $l/h_{tw},$ whereas σ is less significant.

The unimportance of σ can be related to the grade of uniformity of the bed sediments tested. Conversely, the dependence on l/h_{tw} appears surprising, because l was kept constant in this experimental work. Indeed this parameter, although only approximately, probably incorporates the effect of the position of the jump on the apron. It is well known that the flow leaving the apron is charged with turbulence whose intensity will be less when the apron is long downstream of the jump. Then, the distance of the toe of the jump from the apron end would be more appropriate than $l/h_{tw},$ however its determination is not easy and l/h_{tw} will be here considered as a substitute. In particular, the following equations were found to estimate $z, x,$ and χ

$$\frac{z}{h_{tw}} = 0.05 F_d^{2.51} \left(\frac{h_{tw}}{d_{50}} \right)^{-0.51} \left(\frac{l}{h_{tw}} \right)^{0.49} T^{0.15} \quad (9)$$

$$\frac{x}{h_{tw}} = 0.05 F_d^{2.59} \left(\frac{h_{tw}}{d_{50}} \right)^{-0.34} \left(\frac{l}{h_{tw}} \right)^{0.77} T^{0.14} \quad (10)$$

$$\frac{\chi}{h_{tw}} = 0.16 F_d^{2.95} \left(\frac{h_{tw}}{d_{50}} \right)^{-0.43} \left(\frac{l}{h_{tw}} \right)^{0.90} T^{0.12} \quad (11)$$

with $r^2=0.84, 0.87,$ and 0.88 between the observed and the computed values of $z/h_{tw}, x/h_{tw},$ and $\chi/h_{tw},$ respectively. The range of applicability of Equations (9) to (11) is $1.30 \leq F_d \leq 2.87,$ $2.4 \cdot 10^3 \leq T \leq 1.4 \cdot 10^6,$ and $20 \leq h_{tw}/d_{50} \leq 147.$ But additional experiments varying l are needed to identify physically consistent values of the exponent of $l/h_{tw}.$

The above equations do not allow a simple comparison between aprons with and without end-sill. Then, with

reference to runs for $s=0$ (plain apron), the dimensionless variable Ψ was considered as the ratio of a given estimated value according to Equations (9) to (11) to the computed value from Equations (6) to (8) at the same hydraulic conditions (Q and h_{tw}) as the model with the end-sill. Figure 3 shows Ψ_z , Ψ_x , and Ψ_χ as function of the relative submergence h_{tw}/d_{50} with the subscript of Ψ depending on the considered characteristic (either z , x , or χ) of the scour hole. Ψ_x was always found greater than or equal to unity. Then the end-sill forces the location of the maximum scour depth closer to the end of the apron reducing the safety of the structure. Conversely, the apron without end-sill induces overall deeper and longer scour holes. A statistical analysis on Ψ_z and Ψ_χ revealed that they mainly depend on the relative submergence h_{tw}/d_{50} , the relative length of the apron l/h_{tw} and the dimensionless time T . In particular, they decrease as h_{tw}/d_{50} increases, l/h_{tw} decreases, and T increases. Thus, the difference between the behaviour of aprons with and without end-sill tends to vanish under submerged flows. Moreover, the decreasing trend with T , although not as significant as for h_{tw}/d_{50} , is consistent with experimental evidences according to during some runs the toe of the hydraulic jump gradually moved upstream with a consequent reduction of the jet turbulence intensity at the bed inlet. The plots in Figure 3 also reveal that for about $h_{tw}/d_{50} > 100$ Ψ_z and Ψ_χ can be even lower than unity which would imply a some tendency of the end-sill in amplifying the scour magnitude probably due to the deflection of jet.

Geometrical affinity of scour profiles

Farhodi and Smith (1985) demonstrated the similarity of the scour profiles by normalizing both the length and depth of each axial scour profile with respect to z . Conversely, Oliveto *et al.* (2011) did not find experimental evidences in support of this similarity for positive-step stilling basins and a reduction in data scatter was achieved by normalizing the generic length of the scour hole with χ and the generic depth with z resulting in X_χ and Z_z , respectively. In particular, they suggested the following envelope curve

$$Z_z = -0.53 - 3.06X_\chi + 5.50X_\chi^2 - 1.91X_\chi^3. \quad (12)$$

Here a similar analysis as that provided by Oliveto *et al.* (2011) was applied for the plain apron. A few runs were not considered due to the combination of general and local scour which made difficult an accurate determination of χ . The results highlight that affinity, rather than similarity, can be the property of scour profiles. In particular, the following equation was identified

$$Z_z = -0.29 - 4.25X_\chi + 7.28X_\chi^2 - 2.74X_\chi^3. \quad (13)$$

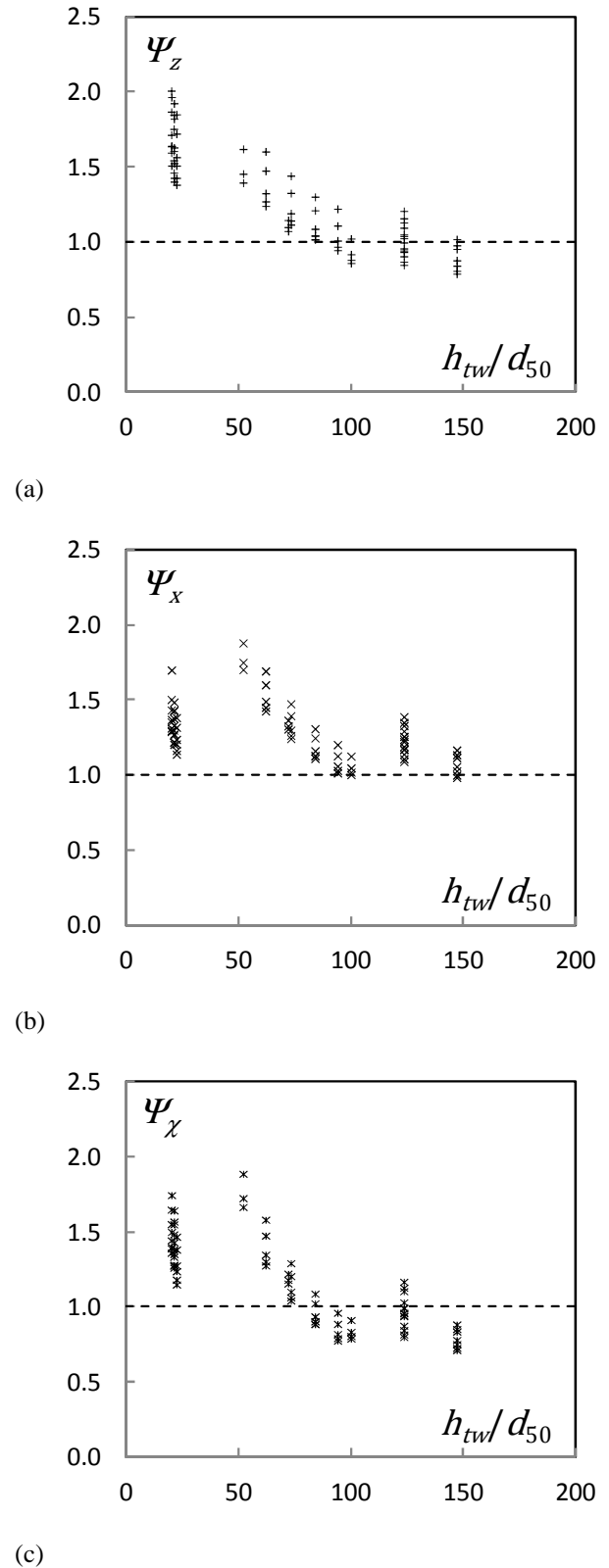


Figure 3: Ratios Ψ_z , Ψ_x , and Ψ_χ as function of the relative submergence h_{tw}/d_{50} for the scour hole characteristics (a) z , (b) x , and (c) χ . Dashed horizontal lines represent Ψ_z , Ψ_x , and $\Psi_\chi=1$.

Finally, Figure 4 compares the experimental data with Equation (13) resulting in a satisfactory (nearly) envelope curve. Moreover, the comparison between the curve of Equation (12) and that of Equation (13) shows as the rising limbs are practically identical while the falling limbs are clearly distinguishable with the curve for the positive-step stilling basins indicating a some propensity of the end-sill in amplifying the scour magnitude just behind the stilling basin end.

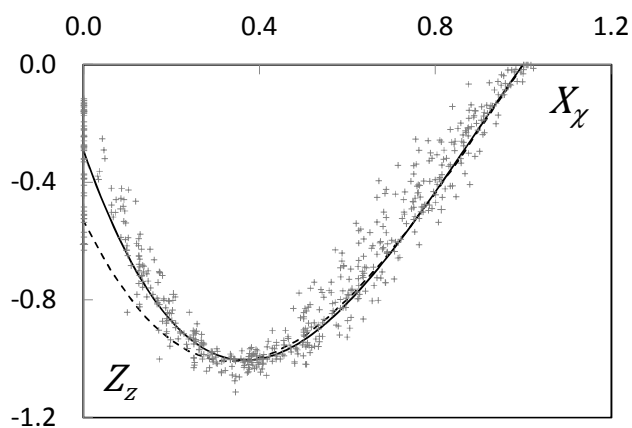


Figure 4: Temporal axial scour profiles normalized with χ (streamwise direction) and z (vertical direction). The full curve represents Equation (13) and dashed curve represents Equation (12).

Conclusions

Laboratory experiments on local scour downstream of low-head stilling basins were carried out. The experiments were addressed to the temporal and spatial evolution of the bed morphology downstream of aprons with and without end-sill. Runs lasted from 1 up to 216 hours and three days on the average to approach nearly equilibrium conditions and well definite scour holes. Four uniform sediments were used, among which lead spheres to better explore the effect of the densimetric Froude number and gravel to better distinguish grain size effects. The main results can be summarized as follows: (i) dimensional analysis leads to the functional relationships (3) to (5) for the prediction of the main scour hole features; (ii) thus, the predictive models (6) to (8) and (9) to (11) were derived from multiple regression analysis. The tailwater densimetric Froude number F_d , the dimensionless time T , and the relative submergence h_{tw}/d_{50} were found as the most significant independent variables. Conversely, the relative stilling basin length, l/h_{tw} , was found less influential as compared to the other variables probably due to the restricted range investigated; (iii) for given hydraulic conditions, the main scour hole dimensions for plain apron were found greater than those for positive-step stilling basins, but decreasing with h_{tw}/d_{50} , h_{tw}/l , and T ; (iv) finally, no experimental

evidences were found in support of the similarity of the axial scour profiles. Conversely, the experimental data collected would reinforce the conjecture of Oliveto and Comuniello (2009) on the geometrical affinity.

References

- Adduce, C., & La Rocca, M. (2006). Local Scouring due to Turbulent Water Jets downstream of a Trapezoidal Drop: Laboratory Experiments and Stability Analysis. *Water Resources Research*, 42(2), W02405.
- Adduce, C., & Sciortino, G. (2006). Scour due to a Horizontal Turbulent Jet: Numerical and Experimental Investigation. *Journal of Hydraulic Research*, 44(5), pp. 663-673.
- Breusers, H.N.C. (1967). Time Scale of Two-Dimensional Local Scour. *Proc. 12th IAHR Congress*, Ft. Collins, USA, Vol. 3, pp. 275-282.
- Breusers, H.N.C., & Raudkivi, A.J. (1991). *Scouring*. Rotterdam: A.A. Balkema.
- Dargahi, J. (2003). Scour Development downstream of a Spillway. *Journal of Hydraulic Research*, 41(4), pp. 417-426.
- Dey, S., & Sarkar, A. (2006). Scour downstream of an Apron due to Submerged Horizontal Jets. *Journal of Hydraulic Engineering*, 132(3), pp. 246-257.
- Farhoudi, J., Hosseini, S.M., & Sedghi-Asl, M. (2010). Application of Neuro-Fuzzy Model to Estimate the Characteristics of Local Scour downstream of Stilling Basins. *Journal of Hydroinformatics*, 12(2), pp. 201-211.
- Farhoudi, J., & Smith, K.V.H. (1982). Time Scale for Scour downstream of Hydraulic Jump. *Journal of Hydraulic Engineering*, 108(10), pp. 1147-1162.
- Farhoudi, J., & Smith, K.V.H. (1985). Local Scour Profiles downstream of Hydraulic Jump. *Journal of Hydraulic Research*, 23(4), pp. 343-358.
- Gisonni, C., & Rasulo, G. (1997). Local Scouring downstream of Positive Step Stilling Basins. *Proc. 27th IAHR Congress*, San Francisco, California, Vol. D, pp. 423-428.
- Hager, W.H. (1992). *Energy dissipators and hydraulic jump*. Dordrecht: Kluwer Academic Publishers.
- Hoffmans, G.J.C.M., & Verheij, H.J. (1997). *Scour Manual*. Rotterdam: A.A. Balkema.
- Kuti, E.O., & Yen, C.-L. (1976). Scouring of Cohesive Soils. *Journal of Hydraulic Research*, 14(3), pp. 195-206.
- Oliveto, G. (2012). Local Scour downstream of a Spillway with an Apron. *Water Management*, submitted.
- Oliveto, G., & Comuniello, V. (2009). Local Scour downstream of Positive-Step Stilling Basins. *Journal of Hydraulic Engineering*, 135(10), pp. 846-851.
- Oliveto, G., Comuniello, V., & Bulbule, T. (2011). Time-Dependent Local Scour downstream of Positive-Step Stilling Basins. *Journal of Hydraulic Research*, 49(1), pp. 105-112.
- Pagliara, S., & Palermo, M. (2011). Effect of Stilling Basin Geometry on Clear Water Scour Morphology downstream of a Block Ramp. *Journal of Irrigation and Drainage Engineering*, 137(9), pp. 593-601.
- Sarkar, A., & Dey, S. (2004). Review on Local Scour due to Jets. *International Journal of Sediment Research*, 19(3), pp. 210-238.